



Article

Novel CaF₂ Nanocomposites with Antibacterial Function and Fluoride and Calcium Ion Release to Inhibit Oral Biofilm and Protect Teeth

Heba Mitwalli ^{1,2}, Abdulrahman A. Balhaddad ^{1,3} , Rashed AlSahafi ^{1,4}, Thomas W. Oates ⁵, Mary Anne S. Melo ^{5,6} , Hockin H. K. Xu ^{5,7,8} and Michael D. Weir ^{5,*}

¹ Program in Dental Biomedical Sciences, University of Maryland School of Dentistry, Baltimore, MD 21201, USA; hmitwalli@umaryland.edu (H.M.); aabalhaddad@umaryland.edu (A.A.B.); rashed.alsahafi@umaryland.edu (R.A.)

² Department of Restorative Dental Science, College of Dentistry, King Saud University, Riyadh 11451, Saudi Arabia

³ Department of Restorative Dental Sciences, College of Dentistry, Imam Abdulrahman bin Faisal University, Dammam 31441, Saudi Arabia

⁴ Department of Restorative Dental Sciences, College of Dentistry, Umm Al-Qura University, Makkah 24211, Saudi Arabia

⁵ Department of Advanced Oral Sciences and Therapeutics, School of Dentistry, University of Maryland, Baltimore, MD 21201, USA; TOates@umaryland.edu (T.W.O.); MMelo@umaryland.edu (M.A.S.M.); HXu2@umaryland.edu (H.H.K.X.)

⁶ Division of Operative Dentistry, Department of General Dentistry, University of Maryland School of Dentistry, Baltimore, MD 21201, USA

⁷ Center for Stem Cell Biology & Regenerative Medicine, University of Maryland School of Medicine, Baltimore, MD 21201, USA

⁸ Marlene and Stewart Greenebaum Cancer Center, University of Maryland School of Medicine, Baltimore, MD 21201, USA

* Correspondence: michael.weir@umaryland.edu

Received: 18 May 2020; Accepted: 28 July 2020; Published: 1 August 2020



Abstract: (1) Background: The objective of this study was to develop a novel dental nanocomposite containing dimethylaminohexadecyl methacrylate (DMAHDM), 2-methacryloyloxyethyl phosphorylcholine (MPC), and nanoparticles of calcium fluoride (nCaF₂) for preventing recurrent caries via antibacterial, protein repellent and fluoride releasing capabilities. (2) Methods: Composites were made by adding 3% MPC, 3% DMAHDM and 15% nCaF₂ into bisphenol A glycidyl dimethacrylate (Bis-GMA) and triethylene glycol dimethacrylate (TEGDMA) (denoted BT). Calcium and fluoride ion releases were evaluated. Biofilms of human saliva were assessed. (3) Results: nCaF₂+DMAHDM+MPC composite had the lowest biofilm colony forming units (CFU) and the greatest ion release; however, its mechanical properties were lower than commercial control composite ($p < 0.05$). nCaF₂+DMAHDM composite had similarly potent biofilm reduction, with mechanical properties matching commercial control composite ($p > 0.05$). Fluoride and calcium ion releases from nCaF₂+DMAHDM were much more than commercial composite. Biofilm CFU on composite was reduced by 4 logs ($n = 9$, $p < 0.05$). Biofilm metabolic activity and lactic acid were also substantially reduced by nCaF₂+DMAHDM, compared to commercial control composite ($p < 0.05$). (4) Conclusions: The novel nanocomposite nCaF₂+DMAHDM achieved strong antibacterial and ion release capabilities, without compromising the mechanical properties. This bioactive nanocomposite is promising to reduce biofilm acid production, inhibit recurrent caries, and increase restoration longevity.

Keywords: dental nanocomposite; calcium fluoride nanoparticles; remineralization; antibacterial; protein repellent; oral biofilm

1. Introduction

Dental resin composites are an excellent material for direct restorations of anterior teeth and in many cases posterior teeth due to their esthetics and ease of placement [1]. Nevertheless, composites are known to accumulate more oral bacterial plaque and biofilm than other direct restorative materials, which could expose the restored tooth to a higher risk for future recurrent caries [2]. Indeed, most failed restorations due to secondary caries are restored with composites [3,4]. The formation of plaque starts with the salivary-acquired pellicle formation. The glycoprotein found in the acquired pellicle promotes bacterial cell adherence. The microbes in the biofilm then produce acids which lowers the pH and lead to mineral loss over time resulting in dissolution of the tooth structure, the formation of caries, and failure of the restoration [5–7]. Unfortunately, currently available commercial composites lack antibacterial properties. Accordingly, efforts were made to overcome the presence of cariogenic bacteria, in an effort to prevent recurrent caries [8].

The incorporation of calcium fluoride nanoparticles ($n\text{CaF}_2$) into composites has the potential to reduce demineralization [9]. Fluoride (F) ions work by stimulating the remineralization and suppressing the oral microorganisms [10,11]. The presence of F ions in the event of demineralization enhances the precipitation of calcium and phosphate ions and forms fluorapatite [$\text{Ca}_5(\text{PO}_4)_3\text{F}$] to protect the tooth surface [12–14]. Fluoride was also shown to have the advantage of reducing bacterial acid production to reduce recurrent caries.

Designing a composite containing calcium fluoride nanoparticles would enhance the fluorapatite deposition in the affected tooth structure. When the tooth structure is subjected to acidic attack by the cariogenic pathogens, calcium and phosphate ions are lost from enamel. Using remineralization approaches to restore the lost minerals is required to enforce and strengthen the tooth structure. Therefore, the composite with calcium fluoride nanoparticles would enhance remineralization and form fluorapatite that is able to resist future acidic challenges. Several studies have demonstrated the ability of forming fluorapatite using nanotechnology [15,16]. In one study, they manufactured fluorapatite nanoparticles and examined its doping with silver ion nanoparticles and evaluated its physical and antimicrobial effects. The results showed 30% inhibition of bacterial growth after 4 h of incubation while maintaining the natural morphology of fluorapatite [15]. In another study, fluorapatite was incorporated into chitosan scaffolds. Fluorapatite maintained its structure, granted antimicrobial effects, and showed osteoconductive capability [16].

Furthermore, the incorporation of antibacterial agents into composites have also been investigated. Imazato et al. integrated 12-methacryloyloxydodecylpyridinium bromide (MDPB) into composites and showed successful antibacterial effects [17–20]. The incorporation of quaternary ammonium polyethylenimine (QPEI) into composites also produced a potent and wide-spectrum antimicrobial effect against salivary microorganisms [21]. Antimicrobial peptides (AMPs) were also demonstrated to have antimicrobial properties by bacterial membrane permeabilization and intracellular targeting [22]. Other studies developed antibacterial agents such as dimethylaminohexadecyl methacrylate (DMAHDM) [23,24] and showed a strong antibiofilm activity without compromising the mechanical properties [25].

Previous studies indicated that the salivary protein accumulation on composite surface could lower the efficiency of “contact-killing” mechanisms [26,27]. Accordingly, efforts were made to improve protein-repellent strategies including the addition of protein-repellent agents such as (2-methacryloyloxyethyl phosphorylcholine, or MPC) into resins [28–30]. This method provided resistance to protein adsorption and bacterial adhesion due to the hydrophilic characteristic of MPC [29,30]. However, to date, there has been no report on the development of a novel bioactive dental composite that contains $n\text{CaF}_2$, DMAHDM, and MPC in combination.

The objectives of this study were to develop a new composite consisting nCaF₂, DMAHDM, and MPC, and to investigate the mechanical, ion release and oral biofilm properties for the first time. The following hypotheses were tested: (1) Adding DMAHDM and MPC into the nCaF₂ composite would have mechanical properties similar to a commercial control composite; (2) Adding DMAHDM and MPC into the nCaF₂ composite would not compromise the F and Ca ion release; and (3) The new bioactive composite would have much less microorganisms, produce less biofilm acid, and have better remineralizing properties than the commercial control composite.

2. Materials and Methods

2.1. Fabrication of Composites

The experimental resin consisted of bisphenol A glycidyl dimethacrylate (BisGMA, Esstech, Essington, PA, USA), and triethylene glycol dimethacrylate (TEGDMA, Esstech) at 50:50 mass ratio. Camphorquinone at 0.2% (Millipore Sigma, Burlington, MA, USA) and 0.8% ethyl 4-N, N-diethylaminobenzoate (Millipore Sigma) were incorporated for photoactivation. The resin is referred to as BT resin. MPC (Millipore Sigma) was added at a mass fraction of 3% and incorporated into the BT resin with magnetic stirring bar at 150 rpm to be dissolved completely into the resin.

The synthesis of DMAHDM was performed using a modified Menshutkin reaction [31]. Briefly, 10 mmol of 2-(dimethylamino) ethyl methacrylate (Millipore Sigma), 10 mmol of 1-bromohexadecane (TCI America, Portland, OR, USA), and 3 g of ethanol were combined in a reaction vessel and then stirred for 24 h at 70 °C. After the evaporation of the solvent and removal of impurities, the DMADHM was collected. DMAHDM was added into the BT resin at a mass fraction of 3% and was stirred using a magnetic stirring bar at 150 rpm until it was completely dissolved into the resin.

The nCaF₂ was manufactured using a spray-dry method as described in previous studies, yielding a mean particle size of 32 nm [9,32–34]. The mass fraction of nCaF₂ incorporated into BT resin was 15%, based on our preliminary study. A previous study tested different concentrations of nCaF₂ in composite and, after long-term water-aging, the composite with 20% nCaF₂ had a flexural strength of 60 MPa [33]. In the present study, 15% nCaF₂ was integrated into the resin to achieve good mechanical strength. Silanized barium boroaluminosilicate glass particles with a mean size of 1.4 μm (Dentsply Sirona, Milford, DE, USA) were incorporated into the BT resin for mechanical enhancement. As a commercial control composite, Heliomolar (Ivoclar Vivadent, Mississauga, ON, Canada) was also tested. Heliomolar contains 66.7% filler mass fraction of ytterbium-trifluoride and nanofillers of 40–200 nm of silica. The following groups were tested (Table 1 summarizes the materials used in the study):

1. Heliomolar (referred to as commercial control (CC));
2. BT Resin + 70% glass (referred to as experimental control (EC));
3. Remineralizing composite: BT + 15% nCaF₂ + 55% glass (referred to as nCaF₂);
4. Antibacterial and remineralizing composite: BT + 15% nCaF₂ + 3% DMAHDM + 55% glass (referred to as nCaF₂+DMAHDM);
5. Protein-repellent and remineralizing composite: BT + 15% nCaF₂ + 3% MPC + 55% glass (referred to as nCaF₂+MPC);
6. Antibacterial, protein-repellent, and remineralizing composite: BT + 15% nCaF₂ + 3% DMAHDM + 3% MPC + 55% glass (referred to as nCaF₂+DMAHDM+MPC).

Table 1. Materials used in the study.

Formulation/Manufacturer	Abbreviation	Fluoride	DMAHDM	MPC
Heliomolar, Ivoclar Vivadent, Mississauga, ON, Canada (Commercial control)	CC	+	-	-
30% BT+70% Glass (Experimental Control)	EC	-	-	-
30% BT+15% nCaF ₂ +55% Glass	nCaF ₂	+	-	-
27% BT+15% nCaF ₂ +3%DMAHDM +55% Glass	nCaF ₂ + DMAHDM	+	+	-
27% BT+15% nCaF ₂ +3% MPC +55% Glass	nCaF ₂ +MPC	+	-	+
24% BT+15% nCaF ₂ +3% DMAHDM +3% MPC+55% Glass	nCaF ₂ +DMAHDM+MPC	+	+	+

2.2. Characterization of nCaF₂

Transmission electron microscopy (TEM, Tecnai T12, FEI, Hillsboro, OR, USA) was used to assess the nanoparticles. Samples were prepared through placing nanoparticles on a perforated copper grid coated by a carbon film. To avoid particle agglomeration, the sample was ultrasonicated for 5 min in acetone prior to deposition. Particle size distribution was measured using a laser diffraction particle size analyzer (SALD-2300, Shimadzu North America, Columbia, MD, USA).

2.3. Mechanical Properties Testing

Each composite paste was mixed in a disposable plastic container using a speed mixer (DAC 150.1 FVZ-K SpeedMixer™, FlackTec Inc., Landrum, SC, USA) at a speed of 2800 rpm for 1 min, and then thoroughly mixed by hand on a plastic slab for 5 min. The paste was then placed in a rectangular mold of 2 × 2 × 25 mm³. Mylar strips were placed on both sides, followed by two glass slides. The specimen was light-cured using a curing unit at 1200 mW/cm² (Labolight DUO, GC America, Alsip, IL, USA) on each side for 1 min [35]. After demolding, the samples were stored in a 100% humidity chamber for 24 h at 37 °C. Flexural strength and elastic modulus were tested at a crosshead-speed of 1 mm/min with a 10 mm span with a three-point flexural test using a computer-controlled universal testing system (Insight 1, MTS, Eden Prairie, MN, USA) [36,37]. Flexural strength and elastic modulus were measured after 24 h of specimen immersion in distilled water at 37 °C. Flexural strength: $S = 3P_{\max}/L(2bh^2)$, where P_{\max} is the fracture load, L is span, b is sample width and h is thickness. Elastic modulus: $E = (P/d) (L^3/[4bh^3])$, where load P was divided by displacement d which is the slope in the linear elastic region. Six specimens were tested for each group ($n = 6$).

2.4. Ca and F Ion Release

The ion releases for all groups containing nCaF₂ were tested. A solution of sodium chloride (NaCl) (133 mmol/L) was buffered with 50 mmol/L HEPES to pH 7 [36,38]. Three specimens of 2 × 2 × 12 mm³ were placed into 50 mL of solution, accommodating a specimen volume/solution ratio of 3.0 mm³/mL, similar to those in previous studies [36,38,39]. The specimen's F and Ca ions release were measured at 1, 2, 4, 7, 14, 21, 28, 35, 42, 49, 56, 63, and 70 days. At every time point, aliquots of 2 mL were collected and substituted by a fresh 2 mL solution of NaCl. The aliquots were investigated for Ca ions by a colorimetric assay using a microplate reader (SpectraMax M5, Molecular Probes, San Jose, CA, USA) as previously described, using known standard and calibration curves [36,38,39]. The F ion release was tested with a F ion selective electrode (Orion, Cambridge, MA, USA). Fluoride standard solutions were measured to form a standard curve. The standard curve was used to establish the F concentration. The F ion concentration measurement was performed by combining 0.5 mL of sample and 0.5 mL of undiluted TISAB solution (Fisher Scientific, Pittsburgh, PA, USA).

2.5. Sample Preparation for Biofilm Tests

The cover of a 96 well plate was used to fabricate composite discs for microbiological experiments yielding samples 0.5 mm in thickness and 8 mm in diameter [31]. Composite paste was placed at each indent in the in 96-well plate cover then covered with Mylar strips and glass slides to form a smooth surface. It was then light cured as described previously and then stored for 24 h at 37 °C. The following day discs were magnetically stirred for 1 h at 100 rpm in distilled water to remove uncured monomers [18,40,41]. The specimens were sterilized using ethylene oxide (Anprolene AN 74i, Andersen Products, Haw River, NC, USA) for 24 and allowed to de-gas for 7 days, following the instructions of the manufacturer.

2.6. Saliva Collection and Dental Plaque Microcosm Biofilm Model

Saliva collection was conducted in accordance with the Declaration of Helsinki, and the protocol was approved by the Institutional Review Board at the University of Maryland Baltimore (IRB #: HP-00050407). The advantage of the dental plaque microcosm biofilm model is the use of an inoculum of human saliva to mimic the heterogeneity and complexity of the bacteria that are present in human dental plaque [18]. An equal amount of saliva was simultaneously gathered from ten healthy contributors with normal dentition, free of active caries, and no antibiotic use within the prior 3 months. Contributors were instructed not to brush their teeth 24 h preceding collection and not to eat or drink 2 h preceding the collection. Subsequently, the collected saliva from all participants was mixed and diluted to 70% in sterile glycerol. Then the saliva–glycerol solution was stored at –80 °C until use [42].

For all biofilm experiments, McBain artificial saliva growth medium was used. McBain medium contained 2.5 g/L Type II mucin (porcine, gastric, Millipore Sigma), 2.0 g/L bacteriological peptone (Becton Dickinson, Sparks, MD, USA), 2.0 g/L tryptone (Becton Dickinson), 0.35 g/L NaCl, 1.0 g/L yeast extract (Fisher Scientific), 0.2 g/L potassium chloride (Millipore Sigma), 0.1 g/L cysteine hydrochloride (Millipore Sigma), 0.2 g/L calcium chloride (Millipore Sigma). The pH of the medium was adjusted to 7 and autoclaved. After cooling the medium, 0.0002 g/L vitamin K₁, 0.001 g/L hemin were added. During biofilm experiments, 2% sucrose solution and the saliva–glycerol solution were used as an inoculum at a ratio of 1:50. The sucrose and inoculum were added to the medium and 1.5 mL of the medium was placed in each well of a 24-well plate containing a composite specimen from each groups. Specimen were incubated in 5% CO₂ at 37 °C for 8 h to permit biofilm growth on the samples. The same procedure was repeated after 8 h without the addition of saliva and incubation occurred again for 16 h. After 16 h the samples were moved to a new 24-well plate which contained fresh medium and sucrose, and was further incubated for 24 h. Composites were exposed to bacterial culture for a total of 48 h, which resulted in reasonably mature dental plaque microcosm biofilms on composites [25,43].

2.7. Biofilm Colony Forming Units (CFU) Counts

Nine discs were prepared for each group. Following the 48 h incubation, the disc samples containing biofilm were transported into a vial filled with 1 mL of cysteine peptone water (CPW). This was vortexed for 5 s then sonicated for 5 min and vortexed again to harvest the biofilm [29]. Serial dilutions of the suspensions of bacteria were prepared and transported to agar plates to grow. The CFU were counted on three different agar plates. To determine total streptococci count, mitis salivarius agar (MSA, Becton Dickinson, Sparks, MD, USA) were used. To determine the growth of mutans streptococci, 0.2 units per mL bacitracin (Millipore Sigma) was added to the mitis salivarius agar (MSB). To evaluate the growth of the total microorganisms, tryptic soy blood agar (TSBA) agar plates were used by adding defibrinated sheep blood to tryptic soy agar (TSA, Becton Dickinson). The agar plates were kept at 37 °C in a 5% CO₂ incubator for 48 h. CFU calculation was based on the colony number and multiplied by the dilution factor [29].

2.8. Biofilms Metabolic Activity Evaluation (MTT)

The MTT (3-[4,5-dimethylthiazol-2-yl]-2,5-diphenyltetrazolium bromide) assay was performed to investigate the biofilm metabolic activity. Following 48 h of incubation, the discs ($n = 9$) were transferred into a clean 24-well plate, then 1 mL of tetrazolium dye was placed to every disc. The discs were then incubated in an incubator of 5% CO₂ at 37 °C. Discs were then transported to another 24-well plate, and 1 mL of dimethyl sulfoxide (DMSO) was added to every disc and incubated for 20 min in a dark room [29,44]. After incubation, 200 µL of the DMSO solution was collected and the absorbance at 540 nm was measured [29,44] using a microplate reader (SpectraMax® M5, Molecular Devices, San Jose, CA, USA).

2.9. Biofilms Lactic Acid Production

Following 48 h incubation, discs ($n = 9$) were moved to a different 24-well plate comprising 1.5 mL buffered-peptone water (BPW) with 0.2% sucrose then incubated for 3 h in a 5% CO₂ incubator at 37 °C to release acids. After 3 h, the BPW solution lactic acid concentrations were measured by recording the absorbance at 340 nm [29,44] using a microplate reader (SpectraMax® M5, Molecular Devices). Standard curves were produced by means of lactic acid standards.

2.10. Scanning Electron Microscopy (SEM) of Biofilms

For biofilm visualization and confirmation of bacterial attachments on composite discs, biofilms formed at 24 h, 48 h, and 96 h were sputter-coated with platinum. Scanning electron microscopy (SEM, Quanta 200, FEI Company, Hillsboro, OR, USA) was used to examine the bacterial accumulation (Figure 7).

3. Statistical Analysis

All data were evaluated with one-way analysis of variance (ANOVA), and post hoc multiple comparison using Tukey's honestly significant difference test was performed. All statistical analysis was completed using the GraphPad Prism 8 software package (GraphPad Software, San Diego, CA, USA) at 0.05 level of significance.

4. Results

A representative TEM image of calcium fluoride (nCaF₂) nanoparticles is shown in Figure 1A. The nanoparticle size distribution ranged from 22 nm to 57 nm, with a mean particle size of 32 nm and is illustrated in Figure 1B.

Flexural strength and elastic modulus of the six composite groups (mean ± sd; $n = 6$) are shown in Figure 2A,B, respectively. The flexural strength was measured after one day of immersion in water at 37 °C. The flexural strength was significantly higher in EC and nCaF₂ composites, when compared to the commercial Heliomolar control ($p < 0.05$). Flexural strength in groups with nCaF₂+DMAHDM and nCaF₂+MPC matched those of Heliomolar control composite ($p > 0.05$). However, flexural strength in nCaF₂+DMAHDM+MPC was significantly lower than commercial Heliomolar control ($p < 0.05$).

The elastic modulus values of EC and nCaF₂ were significantly greater than all other groups ($p < 0.05$). Other groups had comparable elastic modulus values to Heliomolar control ($p < 0.05$).

The accumulative F ion release is shown in Figure 3. At 70 days, the composite nCaF₂+MPC had the highest F release of (0.40 ± 0.02) mmol/L ($p < 0.05$). Meanwhile, nCaF₂+DMAHDM+MPC had F release of (0.25 ± 0.03) mmol/L, nCaF₂+DMAHDM had (0.20 ± 0.03) mmol/L, and nCaF₂ had (0.04 ± 0.01) mmol/L of fluoride ion release. Heliomolar control had the lowest F release of (0.004 ± 0.0003) mmol/L.

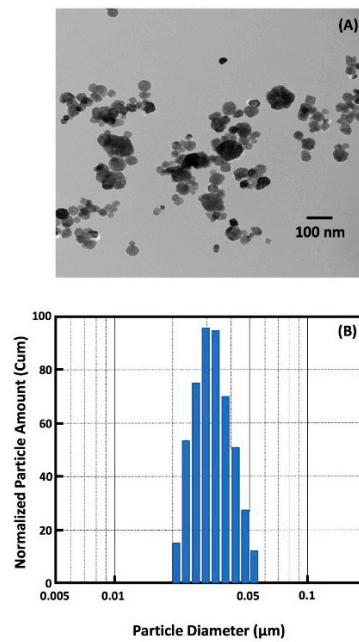


Figure 1. (A) TEM of nanoparticles of CaF₂ (nCaF₂) synthesized in this study. (B) Particle size distribution of nCaF₂. The nCaF₂ were synthesized via a spray-drying technique and collected using an electrostatic precipitator.

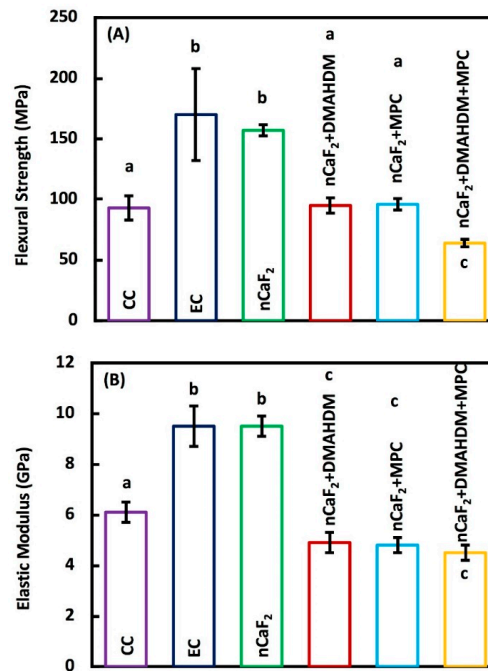


Figure 2. Mechanical properties of composites: (A) Flexural strength, and (B) Elastic modulus (mean ± sd; *n* = 6). The flexural strength was higher in experimental control (EC) and nCaF₂ than commercial Heliomolar control (*p* < 0.05). Flexural strength in nCaF₂+DMAHDM and nCaF₂+MPC matched Heliomolar control (*p* > 0.05). However, the flexural strength in nCaF₂+DMAHDM+MPC was reduced (*p* < 0.05). The elastic modulus of the EC and nCaF₂ were higher than Heliomolar control (*p* < 0.05). All other groups had comparable elastic moduli to Heliomolar control after 1 day of immersion (*p* > 0.05). In each plot, different letters (a, b, c) indicate values that are significantly different from each other (*p* < 0.05).

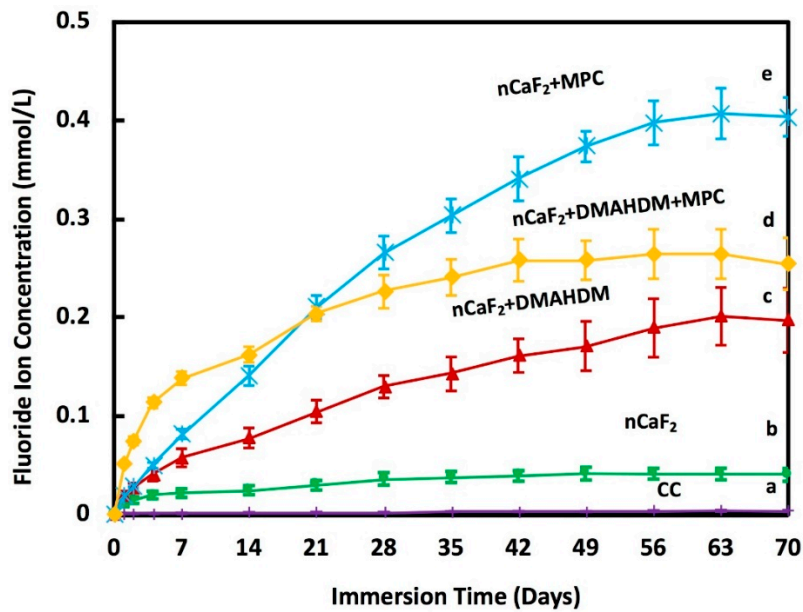


Figure 3. Fluoride (F) ion release from composites (mean ± sd; $n = 6$) at pH 7.0. The incorporation of nCaF₂, DMAHDM, and MPC increased the release of F ions with time ($p < 0.05$). Different letters (a, b, c, d, e) indicate significant differences between groups at day 70 ($p < 0.05$).

The calcium ion release is plotted in Figure 4. At 70 days, nCaF₂+MPC had a Ca ion release of (0.32 ± 0.005) mmol/L, and nCaF₂+DMAHDM+MPC had a similar ion release at (0.35 ± 0.006) mmol/L. Groups containing MPC had ion releases that were significantly higher when compared to other groups ($p < 0.05$). nCaF₂ had a Ca ion release of (0.11 ± 0.004) mmol/L. nCaF₂+DMAHDM had (0.18 ± 0.005) mmol/L, and Heliomolar control had close to zero Ca ion release.

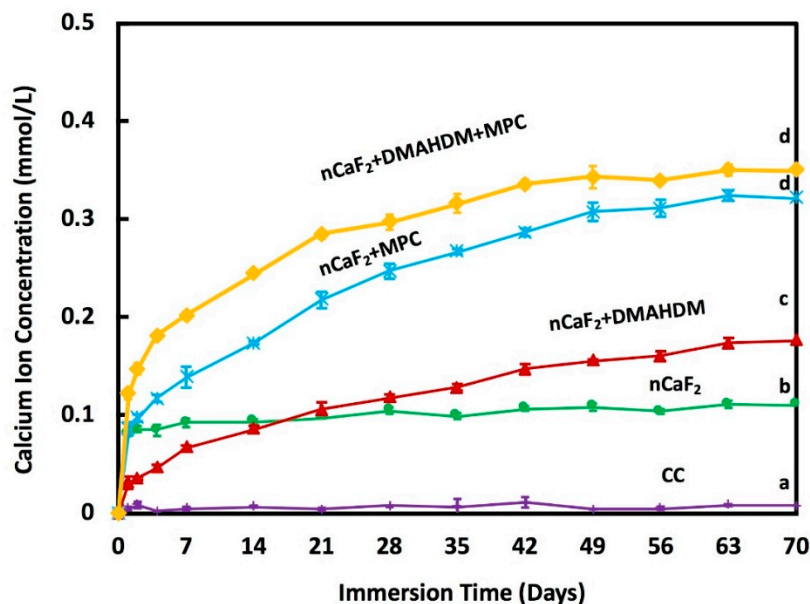


Figure 4. Calcium (Ca) ion release from composite resins (mean ± sd; $n = 6$) at pH 7.0. The incorporation of nCaF₂, DMAHDM, and MPC increased the release of Ca ions with time ($p < 0.05$). Different letters (a, b, c, d) indicate significant differences between groups at day 70 ($p < 0.05$).

Two-day biofilm colony forming units CFU on composites are shown in Figure 5: (A) Total microorganisms, (B) total streptococci and (C) mutans streptococci (mean ± SD; $n = 9$). CFU was reduced by 6 logs from a mean of 2.51×10^8 counts for Heliomolar control to 1.00×10^2 counts for the

new nCaF₂+DMAHDM+MPC composite ($p < 0.05$). nCaF₂+DMAHDM reduced the CFU by 4 logs ($p < 0.05$). The combination of nCaF₂+DMAHDM+MPC yielded the smallest CFU counts.

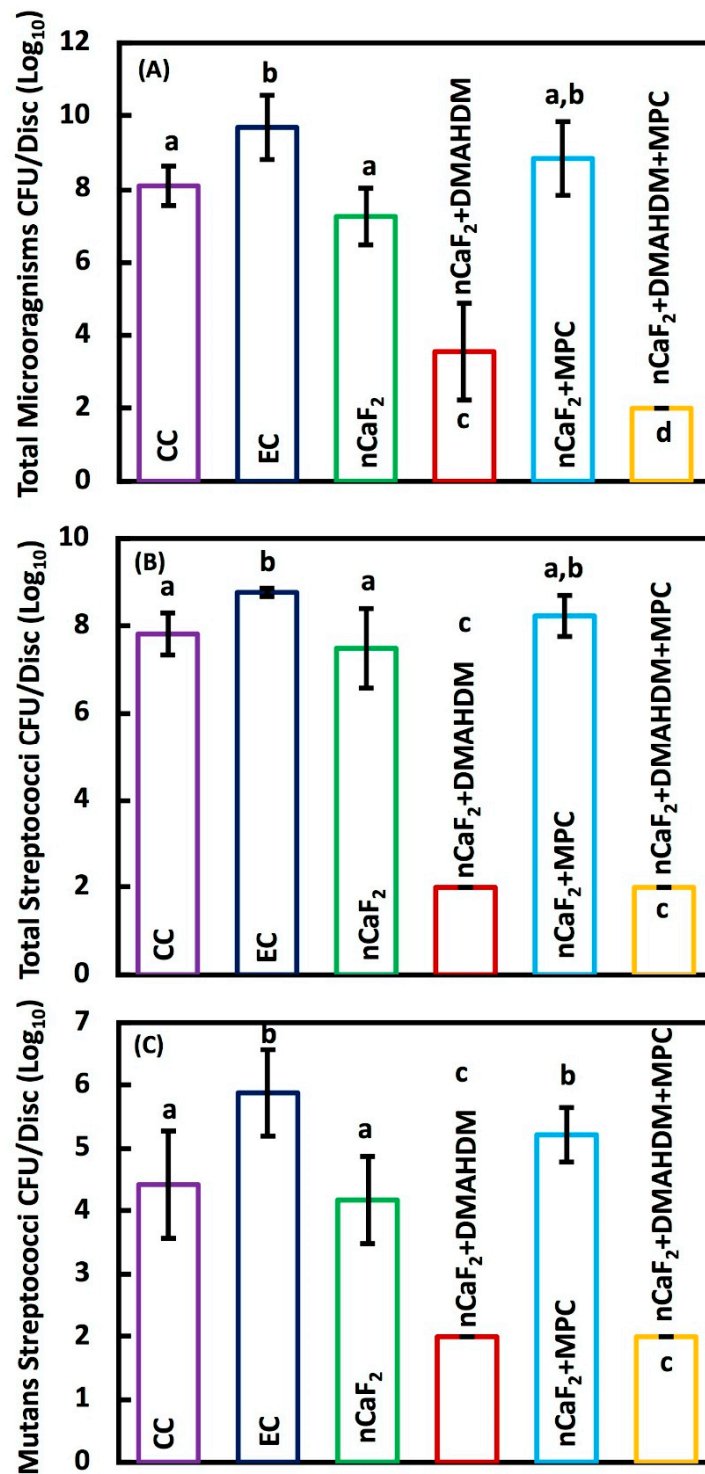


Figure 5. Colony-forming unit (CFU) counts of 2-day biofilm on composite discs (mean \pm sd; $n = 9$): (A) Total microorganisms, (B) total streptococci, and (C) mutans streptococci (mean \pm sd; $n = 9$). The incorporation of nCaF₂+DMAHDM+MPC had the lowest CFU, followed by nCaF₂+DMAHDM in the total microorganisms. The reduction of CFU in nCaF₂+DMAHDM+MPC and nCaF₂+DMAHDM was similar in total streptococci and mutans streptococci ($p < 0.05$). In each plot, different letters (a, b, c, d) indicate significant differences between groups ($p < 0.05$).

The bacterial metabolic activity of 2 days biofilm on composites is shown in Figure 6A. Metabolic activity was decreased from 0.18 (OD_{540}/cm^2) for commercial Heliomolar composite control, to 0.02 for the nCaF₂+DMAHDM+MPC composite ($p < 0.05$). Biofilm lactic acid production results can be seen in Figure 6B. The lactic acid production was reduced from 0.72 mmol/L on commercial Heliomolar control composite to 0.29 mmol/L in the nCaF₂+DMAHDM+MPC composite.

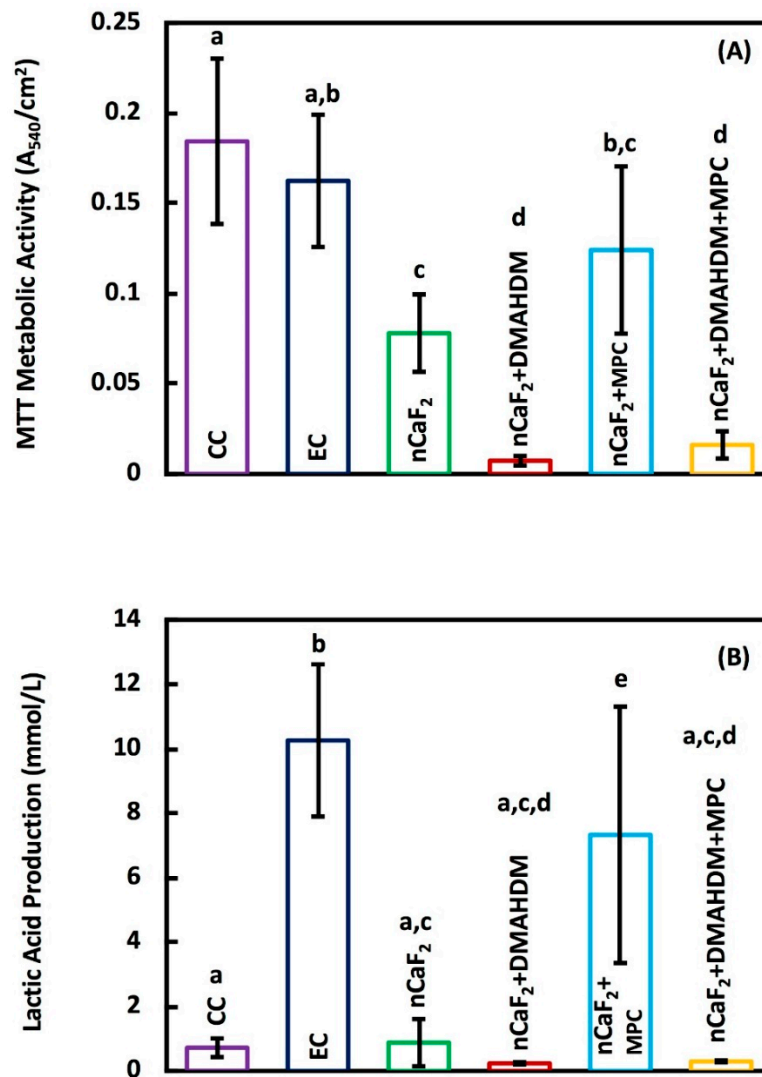


Figure 6. (A) The total metabolic activity, and (B) Lactic acid production (mean \pm sd; $n = 9$) of composite specimens exposed to salivary biofilm. The incorporation of nCaF₂+ DMAHDM had the best reduction in the metabolic activity and lactic acid production ($p < 0.05$). In each plot, different letters (a, b, c, d) indicate significant differences between groups ($p < 0.05$).

SEM results in Figure 7 indicate an extensive biofilm formation at 24 h, 48 h, and 96 h in all groups except those containing the antimicrobial DMAHDM. Heliomolar (CC), experimental control (EC), and nCaF₂+MPC groups had the most biofilm formation at all time points, followed by the nCaF₂ group. Biofilm formation increased with time. However, in DMAHDM-containing groups there was minimal attachment of biofilm observed. At 96 h, the DMAHDM-containing groups showed a reduction in biofilm attachment compared with earlier time points.

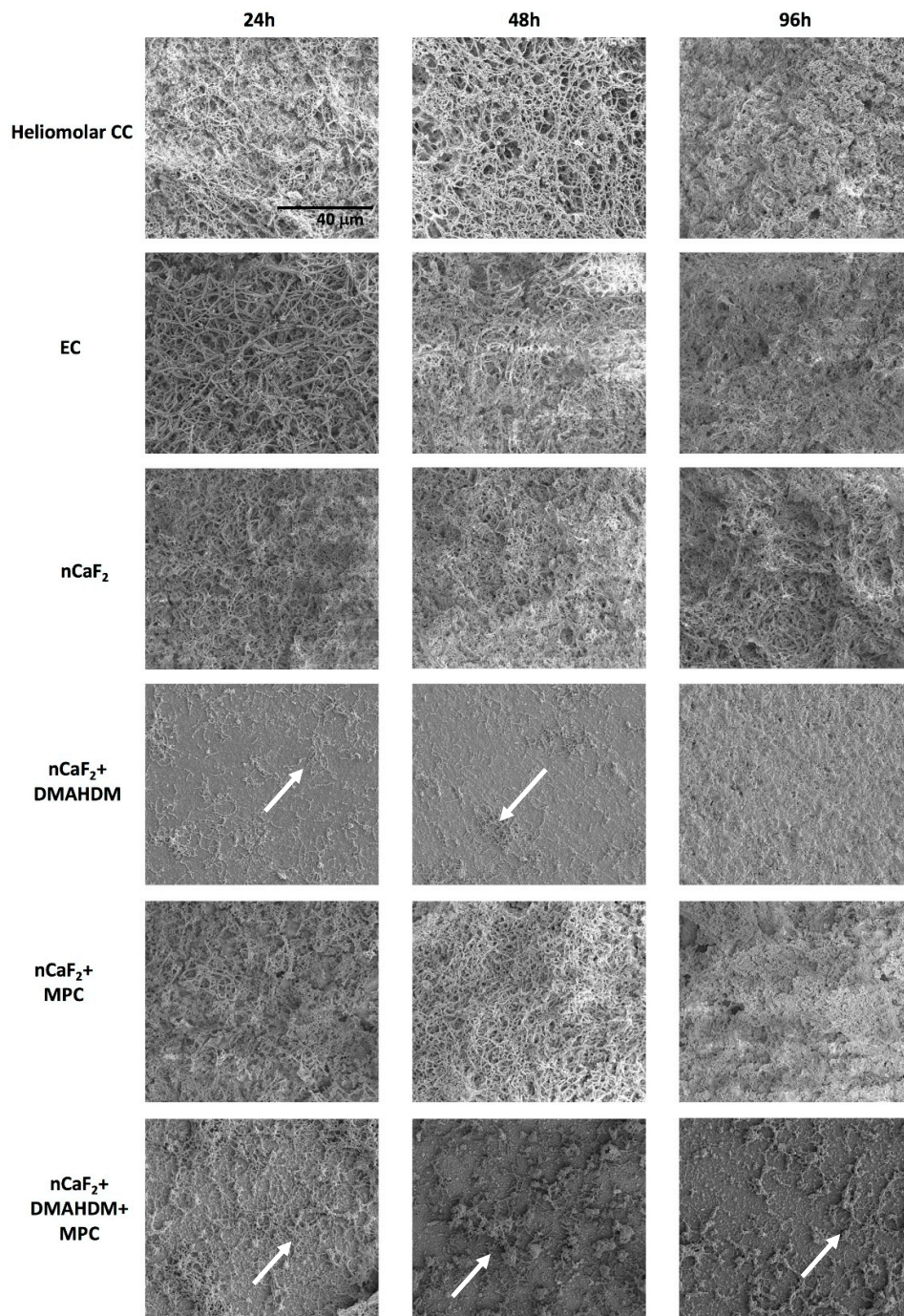


Figure 7. Scanning Electron Microscopy (SEM) images of biofilm formed on composite disc surfaces at 24 h, 48 h, and 96 h. All images are at 3000× magnification. Arrows indicate presence of minimal biofilm on DMAHDM-containing specimens. All other groups had full coverage of a substantial and mature biofilm.

5. Discussion

The present study developed a new composite consisting of nCaF₂, DMAHDM and MPC, and investigated the mechanical, ion release and oral biofilm properties. The protein-repellant nCaF₂+DMAHDM+MPC had slightly lower mechanical properties when compared to all other groups. However, nCaF₂+DMAHDM had good mechanical properties matching those of a commercial composite, while possessing high levels of F and Ca ion release and a strong antibacterial effect.

The new bioactive composite nCaF₂+DMAHDM decreased biofilm CFU by four orders of magnitude over that of commercial control composite, and substantially reduced acid production to inhibit caries.

Critical to the development of any new composite restorative material are its mechanical properties. The flexural strength of EC was around (170 ± 38) MPa. With the addition of 15% nCaF₂, the strength was reduced slightly to (157 ± 5) MPa. Those values are consistent with the results in a previous study [32]. The composite in that study had 65% total fillers and 20% CaF₂, similar to the 70% total fillers and 15% nCaF₂ composition in the present study. The flexural strength for the control group containing no nCaF₂ in the previous study was (145 ± 9) MPa, while the group which had 20% nCaF₂ had a flexural strength of 121 MPa. The nCaF₂+DMAHDM and nCaF₂+MPC had similar strengths of (95 ± 6), and (96 ± 5) MPa, respectively. Meanwhile, for nCaF₂+DMAHDM+MPC, the flexural strength was around (64 ± 3) MPa. Those are similar to the results of a previous study using the same filler mass fraction where the flexural strength was around 90 MPa when 3% MPC and 3% DMAHDM were added to the BT resin [43]. The decreased strength in nCaF₂+DMAHDM+MPC could be due to two reasons. First, the BT base resin is composed of BisGMA and TEGDMA, which contain two reactive groups each. However, both DMAHDM and MPC are monomethacrylates and contain one reactive group. The addition of these monomethacrylates may substantially change the reaction kinetics and resulting crosslinked network, which can result in inferior mechanical properties. Another possible explanation for the decrease in mechanical properties is due to the hydrophilic nature of MPC. The specimens for flexural strength were stored for 24 h in water at 37 °C. The hydrophilicity of MPC makes it more likely that the composite would absorb water during the 24 h immersion prior to testing. This would likely lead to the reduction in flexural strength compared with the non-MPC groups.

Fluoride releasing materials have been known to render teeth more resistant to decay [45]. However, many available materials with fluoride-releasing properties, such as glass ionomer and resin modified glass ionomers, have inferior mechanical properties that do not serve the high load requirements for restorations in stress-bearing areas. Therefore, the incorporation of F ions into composite restorations would have the dual benefit of fluoride release and improved mechanical properties [46–48]. The current study synthesized nCaF₂ through a spray-drying method, which produced nanoparticles of CaF₂ with a median particle size of about 32 nm. The use of small amounts of nCaF₂ fillers prevented the mechanical properties to be compromised. As seen in previous studies, the use of fluoride fillers with larger particle sizes require higher mass fractions of fillers to achieve significant fluoride ion release. This would lead to a decrease in the composite mechanical properties [49].

The incorporation of nanoparticles with a high surface area resulted in the release of high levels of F and Ca ions using a low nCaF₂ filler level [33]. F ions foster remineralization by forming fluoroapatite [Ca₅(PO₄)₃F] [50]. Furthermore, it was shown that the lower the pH, the higher the release of ions. In this study, the release of F ions was significantly increased with the integration of 15% nCaF₂ at a pH of 7, measuring (0.04 ± 0.01) mmol/L. This was comparable to the 0.03 mmol/L F release level in a study that had a pH of 6, yet with an increased percentage of CaF₂ (23%) [51]. Groups containing MPC had the highest F ion release over time. The levels of release in nCaF₂+MPC and nCaF₂+DMAHDM+MPC were (0.40 ± 0.02) mmol/L and (0.25 ± 0.03) mmol/L, respectively. This could be due to the hydrophilic nature of MPC, resulting in a higher level of water uptake. As more water was absorbed by the composite, the Ca and F ions were solubilized, leading to an increase in the initial ion release. However, nCaF₂+DMAHDM F ion release was (0.20 ± 0.03) mmol/L, which was superior to the control. While the amount of nCaF₂ was the same in the two groups, the lower level of initial release in nCaF₂+DMAHDM, when compared to MPC containing groups, could result in a more sustained level of F ion release over a longer period. The releasing trend of F and Ca ions were the same for all groups. The groups containing nCaF₂ had a high F release initially, and subsequently were followed by a steady state release. The higher release of Ca and F ions in all nCaF₂ composites revealed that CaF₂ nanoparticles were fast released from the nCaF₂ composites because of the hydrolytic breakdown of the interface between the resin matrix and the CaF₂ nanoparticles. A likely explanation for such a trend is that the ions were released from the near-surface Ca and F reservoir of the nCaF₂ composite, and the reservoir

near the surface diminished with the increase in immersion time. However, in clinical situations, the superficial layer of nCaF₂ would experience repeated chewing forces and tooth-brushing, hence the CaF₂-depleted surface would be removed by wear. As a result, a fresh surface would be exposed with the ability to further continue the calcium and fluoride release. Further studies are needed to investigate the outcome of wear on Ca and F ion release, as well as whether these materials can be made rechargeable to extend the lifetime of ion release.

Recurrent caries is considered a major drawback of composite restorations [1,52,53]. Studies proposed that the greater vulnerability to recurrent caries may be associated with the absence of composites' antibacterial capability when compared to other commonly used restorative materials such as glass ionomers and amalgams [2,54]. Therefore, the improvement of composites by incorporating antibacterial, protein repellent, and remineralizing properties is essential to lengthen the service life of composite restorations. DMAHDM has demonstrated strong antibacterial effects on an extensive antimicrobial spectrum through its contact-killing properties [26,55]. Since DMAHDM contains a reactive methacrylate group, it is copolymerized within the resin matrix, rendering it immobilized and preventing its release or loss over time [26,56]. Hence, its antibacterial capability is long-lasting. However, the antibacterial ability of DMAHDM is limited to biofilms that contact the composite surface [26], as biofilms that are not in contact with DMAHDM cannot be killed via DMAHDM's mechanism of action. Even with this limitation, the composite containing nCaF₂+DMAHDM substantially lowered the biofilm development and production of lactic acid, reducing the CFU of biofilm by 4 logs.

It can be seen in Figure 6B that the experimental control group and the group containing nCaF₂ and MPC exhibited a greater lactic acid production when compared with the other groups. DMAHDM has been shown in previous work to have a strong antibacterial effect, as illustrated by the CFU data in Figure 5. This antibacterial activity is reflected indirectly by the lactic acid production. When an *S mutans* biofilm accumulates, the secretion of lactic acid occurs. In the absence of a viable biofilm, the concentration of lactic acid is expected to be very low, as is the case in the DMAHDM-containing groups. Interestingly, the nCaF₂ and nCaF₂+MPC groups did not have a significant reduction in CFU (Figure 5), but the nCaF₂ group showed a significant reduction in lactic acid production in contrast to the nCaF₂+MPC group. Previously, it has been shown that the inclusion of CaF₂ in a composite formulation has a moderating effect on the lactic acid production [57]. It has been speculated that the F ion release helped reduce the acid production of the bacteria via the inhibition of metabolic pathways such as the fermentation pathway for lactic acid production, biofilm plaque, and hydrodynamic effects on mass transfer, fluoride delivery, and caries [58]. However, when MPC was added to the composite containing nCaF₂, there was no decrease in lactic acid production. This response may be related to the interactions between the calcium and fluoride ions and the phosphorylcholine fragment of MPC. The protein-repellent nature of MPC from the hydrogen bond network of water molecules surrounding the phosphorylcholine fragment limited the ability of the protein to adsorb on the surface. It was found, however, that the presence of halide ions (Cl⁻, Br⁻, I⁻) influenced the hydrogen bond network and the diffusion through it [59]. It is possible that the presence of F⁻ ions would have a similar result, which may affect F ion diffusion and disrupt the creation of a protein-repellant coating, leading to biofilm formation.

SEM images in Figure 7 confirm the presence of substantial biofilm on all groups except those containing DMAHDM. At 24 h and 48 h, Heliomolar (CC), experimental control (EC), nCaF₂, and nCaF₂+MPC groups exhibited the formation of microcolonies and early biofilm multilayers. The biofilms on these groups at 96 h were fully mature, substantial, and dense. However, in DMAHDM-containing groups there was minimal attachment of biofilm observed. At 96 h the DMAHDM-containing groups showed a reduction in biofilm attachment compared to earlier time points. It is possible that the antimicrobial effect of DMAHDM as a contact-killing agent had eliminated the bacteria left on the samples over time. These results correlate very well with the CFU results.

It is possible that the salivary proteins adsorption on composite resin surfaces might reduce the effectiveness of this “contact-killing” mechanism. Therefore, a protein repellent agent was added. MPC is a methacrylate that contains phospholipid polar groups. MPC is highly hydrophilic and has been shown to decrease the adsorption of protein and reduce bacterial attachments [60]. Previous work indicated that integrating MPC into the resin decreased the adsorption of proteins by approximately one order of magnitude [43,61]. Additionally, it was shown that surfaces containing MPC were resistant to brushing mechanical stresses [62]. In this study, MPC was incorporated into the resin, and copolymerized into the composite resin. This is analogous to the process of incorporating DMAHDM, with a similar result of a stable, covalently bonded, and non-releasing functionality.

In the current study, the antibacterial capability of the experimental composite was improved with nCaF₂ and was further substantially improved with the use of both nCaF₂ and DMAHDM. However, the nCaF₂+MPC group showed no reduction in the CFU counts. The composite that had nCaF₂+DMAHDM+MPC displayed the most potent antibacterial effect with CFU 6 log biofilm reduction. Therefore, these results confirmed that the addition of DMAHDM is vital to improving the antibacterial effect. It is thought that DMAHDM serves to reduce the accumulation of biofilm and, as a result, improves the efficacy of MPC in resisting protein adsorption. However, in the absence of DMAHDM, the bacterial biofilm will accumulate and render MPC less effective.

The combination of nCaF₂+DMAHDM promoted remineralization and had a significant antibacterial effect. Another potential benefit of using nCaF₂ is that the release of F ions could act as a transmembrane proton carrier and an inhibitor to the glycolytic enzyme, thus preventing oral microorganisms by stimulating acidification of the cytoplasm and providing antibacterial effect at a long-distance to inhibit caries [10,63]. These properties would be highly valuable to inhibit recurrent caries around the margins of the restoration, since this is the location that most dental plaque tends to accumulate. In addition to its superior antibacterial and remineralization properties, the nCaF₂+DMAHDM composite exhibits excellent mechanical properties which make it suitable in a variety of restoration applications. In comparison, the composite consisting of nCaF₂+DMAHDM+MPC exhibited lower mechanical properties. However, the strength and modulus achieved by this group was still high enough to be used for restorations in low load areas such as class V restorations [37]. This is a critical area of utilization, since older patients tend to have exposed root surfaces that are more prone to caries. Further studies are needed to investigate the nCaF₂+DMAHDM combination in dental cements, bonding agents, fissure sealants, and composites to remineralize tooth lesions and suppress biofilm and plaque buildup, especially in patients with a high caries risk.

6. Conclusions

A novel composite with remineralization and antibacterial properties was established by combining nCaF₂+DMAHDM for the first time. Release of F and Ca ions from the composite was significantly achieved through the incorporation of nCaF₂. The new composite exhibited strong antibacterial and ion release capabilities, prevented biofilm production of lactic acid, and decreased biofilm CFU by 4 log. This bioactive nanocomposite is promising to protect tooth structures, inhibit demineralization, and provide a reservoir for the release of calcium and fluoride ions. The combined effect of nCaF₂+DMAHDM shows promise in a variety of dental applications where remineralization and prevention of recurrent caries is a priority.

Author Contributions: H.M. contributed to design, data acquisition, and analysis, and drafted the manuscript; A.A.B. contributed to data acquisition, and analysis; R.A. contributed to data acquisition and analysis; T.W.O. contributed to data interpretation and funding acquisition; M.A.S.M. contributed to data acquisition, analysis, and interpretation; H.H.K.X. contributed to conception, design, data interpretation and critically revised the manuscript; M.D.W. contributed to design, data acquisition, analysis, and interpretation, and critically revised the manuscript. All authors have read and agreed to the published version of the manuscript.

Funding: This research received no external funding.

Acknowledgments: We thank Quan Dai, Jianghong Gao, Maria Ibrahim, Bashayer Baras, Pei Feng, Nancy J. Lin, Jirun Sun, and Laurence C. Chow for discussions and assistance. We thank the technical support of the Core Imaging Facility of the University of Maryland Baltimore. We are grateful to Dentsply Sirona (Milford, DE) for the donation of the glass fillers. This work was supported by The University of Maryland School of Dentistry bridge fund (HX) and University of Maryland seed grant (HX).

Conflicts of Interest: The authors declare no conflict of interest.

References

1. Ferracane, J.L. Resin composite—State of the art. *Dent. Mater.* **2011**, *27*, 29–38. [[CrossRef](#)]
2. Beyth, N.; Domb, A.J.; Weiss, E.I. An in vitro quantitative antibacterial analysis of amalgam and composite resins. *J. Dent.* **2007**, *35*, 201–206. [[CrossRef](#)] [[PubMed](#)]
3. Deligeorgi, V.; Mjör, I.A.; Wilson, N.H. An overview of reasons for the placement and replacement of restorations. *Prim. Dent. Care* **2001**, *8*, 5–11. [[CrossRef](#)] [[PubMed](#)]
4. Jokstad, A.; Bayne, S.; Blunck, U.; Tyas, M.; Wilson, N. Quality of dental restorations. FDI Commission Project 2-95. *Int. Dent. J.* **2001**, *51*, 117–158. [[CrossRef](#)]
5. Takahashi, N.; Nyvad, B. Ecological Hypothesis of Dentin and Root Caries. *Caries Res.* **2016**, *50*, 422–431. [[CrossRef](#)]
6. Kidd, E.A.M.; Fejerskov, O. What constitutes dental caries? Histopathology of carious enamel and dentin related to the action of cariogenic biofilms. *J. Dent. Res.* **2004**, *83*, C35–C38. [[CrossRef](#)]
7. Kidd, E. *Essentials of Dental Caries: The Disease and Its Management*, 3rd ed.; OUP Oxford: Oxford, UK, 2005; ISBN 978-0-19-852978-1.
8. Xu, X.; Ling, L.; Wang, R.; Burgess, J.O. Formulation and characterization of a novel fluoride-releasing dental composite. *Dent. Mater.* **2006**, *22*, 1014–1023. [[CrossRef](#)]
9. Xu, H.H.K.; Moreau, J.L.; Sun, L.; Chow, L.C. Novel CaF₂ Nanocomposite with High Strength and Fluoride Ion Release. *J. Dent. Res.* **2010**, *89*, 739–745. [[CrossRef](#)]
10. Zheng, X.; Cheng, X.; Wang, L.; Qiu, W.; Wang, S.; Zhou, Y.; Li, M.; Li, Y.; Cheng, L.; Li, J.; et al. Combinatorial effects of arginine and fluoride on oral bacteria. *J. Dent. Res.* **2015**, *94*, 344–353. [[CrossRef](#)]
11. Koo, H. Strategies to enhance the biological effects of fluoride on dental biofilms. *Adv. Dent. Res.* **2008**, *20*, 17–21. [[CrossRef](#)]
12. Rošin-Grget, K. The cariostatic mechanisms of fluoride. *Acta Med. Acad.* **2013**, *42*, 179–188. [[CrossRef](#)]
13. ten Cate, J.M. Current concepts on the theories of the mechanism of action of fluoride. *Acta Odontol. Scand.* **1999**, *57*, 325–329. [[CrossRef](#)]
14. ten Cate, J.M. Contemporary perspective on the use of fluoride products in caries prevention. *Br. Dent. J.* **2013**, *214*, 161–167. [[CrossRef](#)]
15. Wojnarowska-Nowak, R.; Rzeszutko, J.; Barylyak, A.; Nechyporenko, G.; Zinchenko, V.; Leszczyńska, D.; Bobitski, Y.; Kus-Liškiewicz, M. Structural, physical and antibacterial properties of pristine and Ag+ doped fluoroapatite nanomaterials. *Adv. Appl. Ceram.* **2017**, *116*, 108–117. [[CrossRef](#)]
16. Anastasiou, A.D.; Nerantzaki, M.; Gounari, E.; Duggal, M.S.; Giannoudis, P.V.; Jha, A.; Bikiaris, D. Antibacterial properties and regenerative potential of Sr²⁺ and Ce³⁺ doped fluorapatites; a potential solution for peri-implantitis. *Sci. Rep.* **2019**, *9*. [[CrossRef](#)]
17. Imazato, S.; Russell, R.R.; McCabe, J.F. Antibacterial activity of MDPB polymer incorporated in dental resin. *J. Dent.* **1995**, *23*, 177–181. [[CrossRef](#)]
18. Imazato, S.; Ehara, A.; Torii, M.; Ebisu, S. Antibacterial activity of dentine primer containing MDPB after curing. *J. Dent.* **1998**, *26*, 267–271. [[CrossRef](#)]
19. Imazato, S. Bio-active restorative materials with antibacterial effects: New dimension of innovation in restorative dentistry. *Dent. Mater. J.* **2009**, *28*, 11–19. [[CrossRef](#)]
20. Imazato, S.; Torii, M.; Tsuchitani, Y.; McCabe, J.F.; Russell, R.R. Incorporation of bacterial inhibitor into resin composite. *J. Dent. Res.* **1994**, *73*, 1437–1443. [[CrossRef](#)]
21. Beyth, N.; Yudovin-Farber, I.; Perez-Davidi, M.; Domb, A.J.; Weiss, E.I. Polyethyleneimine nanoparticles incorporated into resin composite cause cell death and trigger biofilm stress in vivo. *Proc. Natl. Acad. Sci. USA* **2010**, *107*, 22038–22043. [[CrossRef](#)]
22. Jiao, Y.; Tay, F.R.; Niu, L.-N.; Chen, J.-H. Advancing antimicrobial strategies for managing oral biofilm infections. *Int. J. Oral Sci.* **2019**, *11*, 28. [[CrossRef](#)] [[PubMed](#)]

23. Imazato, S. Antibacterial properties of resin composites and dentin bonding systems. *Dent. Mater.* **2003**, *19*, 449–457. [[CrossRef](#)]
24. Faust, D.; Dolado, I.; Cuadrado, A.; Oesch, F.; Weiss, C.; Nebreda, A.R.; Dietrich, C. p38alpha MAPK is required for contact inhibition. *Oncogene* **2005**, *24*, 7941–7945. [[CrossRef](#)] [[PubMed](#)]
25. Li, F.; Weir, M.D.; Xu, H.H.K. Effects of quaternary ammonium chain length on antibacterial bonding agents. *J. Dent. Res.* **2013**, *92*, 932–938. [[CrossRef](#)]
26. Beyth, N.; Yudovin-Farber, I.; Bahir, R.; Domb, A.J.; Weiss, E.I. Antibacterial activity of dental composites containing quaternary ammonium polyethylenimine nanoparticles against *Streptococcus mutans*. *Biomaterials* **2006**, *27*, 3995–4002. [[CrossRef](#)]
27. Namba, N.; Yoshida, Y.; Nagaoka, N.; Takashima, S.; Matsuura-Yoshimoto, K.; Maeda, H.; Van Meerbeek, B.; Suzuki, K.; Takashiba, S. Antibacterial effect of bactericide immobilized in resin matrix. *Dent. Mater.* **2009**, *25*, 424–430. [[CrossRef](#)]
28. Müller, R.; Eidt, A.; Hiller, K.-A.; Katur, V.; Subat, M.; Schweikl, H.; Imazato, S.; Ruhl, S.; Schmalz, G. Influences of protein films on antibacterial or bacteria-repellent surface coatings in a model system using silicon wafers. *Biomaterials* **2009**, *30*, 4921–4929. [[CrossRef](#)]
29. Xie, X.; Wang, L.; Xing, D.; Zhang, K.; Weir, M.D.; Liu, H.; Bai, Y.; Xu, H.H.K. Novel dental adhesive with triple benefits of calcium phosphate recharge, protein-repellent and antibacterial functions. *Dent. Mater.* **2017**, *33*, 553–563. [[CrossRef](#)]
30. Zhang, N.; Weir, M.D.; Romberg, E.; Bai, Y.; Xu, H.H.K. Development of novel dental adhesive with double benefits of protein-repellent and antibacterial capabilities. *Dent. Mater.* **2015**, *31*, 845–854. [[CrossRef](#)]
31. Zhou, H.; Li, F.; Weir, M.D.; Xu, H.H.K. Dental plaque microcosm response to bonding agents containing quaternary ammonium methacrylates with different chain lengths and charge densities. *J. Dent.* **2013**, *41*, 1122–1131. [[CrossRef](#)]
32. Xu, H.H.K.; Moreau, J.L.; Sun, L.; Chow, L.C. Strength and fluoride release characteristics of a calcium fluoride based dental nanocomposite. *Biomaterials* **2008**, *29*, 4261–4267. [[CrossRef](#)] [[PubMed](#)]
33. Weir, M.D.; Moreau, J.L.; Levine, E.D.; Strassler, H.D.; Chow, L.C.; Xu, H.H.K. Nanocomposite containing CaF₂ nanoparticles: Thermal cycling, wear and long-term water-aging. *Dent. Mater.* **2012**, *28*, 642–652. [[CrossRef](#)] [[PubMed](#)]
34. Sun, L.; Chow, L.C. Preparation and properties of nano-sized calcium fluoride for dental applications. *Dent. Mater.* **2008**, *24*, 111–116. [[CrossRef](#)]
35. Trujillo-Lemon, M.; Ge, J.; Lu, H.; Tanaka, J.; Stansbury, J.W. Dimethacrylate derivatives of dimer acid. *J. Polym. Sci. Part A Polym. Chem.* **2006**, *44*, 3921–3929. [[CrossRef](#)]
36. Xu, H.H.K.; Moreau, J.L.; Sun, L.; Chow, L.C. Nanocomposite containing amorphous calcium phosphate nanoparticles for caries inhibition. *Dent. Mater.* **2011**, *27*, 762–769. [[CrossRef](#)]
37. ISO 4049:2009. *Dentistry—Polymer-Based Restorative Materials*; International Organization for Standardization: Geneva, Switzerland, 2009.
38. Xu, H.H.K.; Weir, M.D.; Sun, L.; Takagi, S.; Chow, L.C. Effects of calcium phosphate nanoparticles on Ca-PO₄ composite. *J. Dent. Res.* **2007**, *86*, 378–383. [[CrossRef](#)]
39. Skrtic, D.; Antonucci, J.M.; Eanes, E.D. Improved properties of amorphous calcium phosphate fillers in remineralizing resin composites. *Dent. Mater.* **1996**, *12*, 295–301. [[CrossRef](#)]
40. Wang, L.; Xie, X.; Li, C.; Liu, H.; Zhang, K.; Zhou, Y.; Chang, X.; Xu, H.H.K. Novel bioactive root canal sealer to inhibit endodontic multispecies biofilms with remineralizing calcium phosphate ions. *J. Dent.* **2017**, *60*, 25–35. [[CrossRef](#)]
41. Xie, X.; Wang, L.; Xing, D.; Arola, D.D.; Weir, M.D.; Bai, Y.; Xu, H.H.K. Protein-repellent and antibacterial functions of a calcium phosphate rechargeable nanocomposite. *J. Dent.* **2016**, *52*, 15–22. [[CrossRef](#)]
42. McBain, A.J. In Vitro Biofilm Models: An Overview. In *Advances in Applied Microbiology*; Elsevier: Cambridge, MA, USA, 2009; Volume 69, pp. 99–132.
43. Zhang, N.; Ma, J.; Melo, M.A.S.; Weir, M.D.; Bai, Y.; Xu, H.H.K. Protein-repellent and antibacterial dental composite to inhibit biofilms and caries. *J. Dent.* **2015**, *43*, 225–234. [[CrossRef](#)]
44. Al-Dulaijan, Y.A.; Cheng, L.; Weir, M.D.; Melo, M.A.S.; Liu, H.; Oates, T.W.; Wang, L.; Xu, H.H.K. Novel rechargeable calcium phosphate nanocomposite with antibacterial activity to suppress biofilm acids and dental caries. *J. Dent.* **2018**, *72*, 44–52. [[CrossRef](#)] [[PubMed](#)]

45. Deng, D.M.; van Loveren, C.; ten Cate, J.M. Caries-preventive agents induce remineralization of dentin in a biofilm model. *Caries Res.* **2005**, *39*, 216–223. [[CrossRef](#)] [[PubMed](#)]
46. Kus-Liśkiewicz, M.; Rzeszutko, J.; Bobitski, Y.; Barylyak, A.; Nechyporenko, G.; Zinchenko, V.; Zebrowski, J. Alternative Approach for Fighting Bacteria and Fungi: Use of Modified Fluorapatite. *J. Biomed. Nanotechnol.* **2019**, *15*, 848–855. [[CrossRef](#)] [[PubMed](#)]
47. Montazeri, N.; Jahandideh, R.; Biazar, E. Synthesis of fluorapatite–hydroxyapatite nanoparticles and toxicity investigations. *Int. J. Nanomed.* **2011**, *6*, 197–201. [[CrossRef](#)]
48. Wiegand, A.; Buchalla, W.; Attin, T. Review on fluoride-releasing restorative materials—Fluoride release and uptake characteristics, antibacterial activity and influence on caries formation. *Dent. Mater.* **2007**, *23*, 343–362. [[CrossRef](#)]
49. Balhaddad, A.A.; Kansara, A.A.; Hidan, D.; Weir, M.D.; Xu, H.H.K.; Melo, M.A.S. Toward dental caries: Exploring nanoparticle-based platforms and calcium phosphate compounds for dental restorative materials. *Bioact. Mater.* **2019**, *4*, 43–55. [[CrossRef](#)]
50. Lata, S.; Varghese, N.O.; Varughese, J.M. Remineralization potential of fluoride and amorphous calcium phosphate-casein phospho peptide on enamel lesions: An in vitro comparative evaluation. *J. Conserv. Dent.* **2010**, *13*, 42–46. [[CrossRef](#)]
51. Anusavice, K.J.; Zhang, N.-Z.; Shen, C. Effect of CaF₂ content on rate of fluoride release from filled resins. *J. Dent. Res.* **2005**, *84*, 440–444. [[CrossRef](#)]
52. Sakaguchi, R.L. Review of the current status and challenges for dental posterior restorative composites: Clinical, chemistry, and physical behavior considerations. Summary of discussion from the Portland Composites Symposium (POCOS) June 17–19, 2004, Oregon Health and Science University, Portland, Oregon. *Dent. Mater.* **2005**, *21*, 3–6. [[CrossRef](#)]
53. Demarco, F.F.; Corrêa, M.B.; Cenci, M.S.; Moraes, R.R.; Opdam, N.J.M. Longevity of posterior composite restorations: Not only a matter of materials. *Dent. Mater.* **2012**, *28*, 87–101. [[CrossRef](#)]
54. Nedeljkovic, I.; Teughels, W.; De Munck, J.; Van Meerbeek, B.; Van Landuyt, K.L. Is secondary caries with composites a material-based problem? *Dent. Mater.* **2015**, *31*, e247–e277. [[CrossRef](#)] [[PubMed](#)]
55. Imazato, S.; Ebi, N.; Takahashi, Y.; Kaneko, T.; Ebisu, S.; Russell, R.R.B. Antibacterial activity of bactericide-immobilized filler for resin-based restoratives. *Biomaterials* **2003**, *24*, 3605–3609. [[CrossRef](#)]
56. Xu, X.; Wang, Y.; Liao, S.; Wen, Z.T.; Fan, Y. Synthesis and characterization of antibacterial dental monomers and composites. *J. Biomed. Mater. Res. Part B Appl. Biomater.* **2012**, *100B*, 1151–1162. [[CrossRef](#)]
57. Cheng, L.; Weir, M.D.; Xu, H.H.K.; Kraigsley, A.M.; Lin, N.J.; Lin-Gibson, S.; Zhou, X. Antibacterial and physical properties of calcium-phosphate and calcium-fluoride nanocomposites with chlorhexidine. *Dent. Mater.* **2012**, *28*, 573–583. [[CrossRef](#)]
58. Stoodley, P.; Wefel, J.; Gieseke, A.; Debeer, D.; von Ohle, C. Biofilm plaque and hydrodynamic effects on mass transfer, fluoride delivery and caries. *J. Am. Dent. Assoc.* **2008**, *139*, 1182–1190. [[CrossRef](#)]
59. Zhang, Z.J.; Madsen, J.; Warren, N.J.; Mears, M.; Leggett, G.J.; Lewis, A.L.; Geoghegan, M. Influence of salt on the solution dynamics of a phosphorylcholine-based polyzwitterion. *Eur. Polym. J.* **2017**, *87*, 449–457. [[CrossRef](#)]
60. Sibarani, J.; Takai, M.; Ishihara, K. Surface modification on microfluidic devices with 2-methacryloyloxyethyl phosphorylcholine polymers for reducing unfavorable protein adsorption. *Colloids Surf. B Biointerfaces* **2007**, *54*, 88–93. [[CrossRef](#)]
61. Zhang, N.; Chen, C.; Melo, M.A.; Bai, Y.-X.; Cheng, L.; Xu, H.H. A novel protein-repellent dental composite containing 2-methacryloyloxyethyl phosphorylcholine. *Int. J. Oral Sci.* **2015**, *7*, 103–109. [[CrossRef](#)]
62. Tateishi, T.; Kyomoto, M.; Kakinoki, S.; Yamaoka, T.; Ishihara, K. Reduced platelets and bacteria adhesion on poly(ether ether ketone) by photoinduced and self-initiated graft polymerization of 2-methacryloyloxyethyl phosphorylcholine. *J. Biomed. Mater. Res. A* **2014**, *102*, 1342–1349. [[CrossRef](#)]
63. Van Loveren, C. Antimicrobial activity of fluoride and its in vivo importance: Identification of research questions. *Caries Res.* **2001**, *35* (Suppl. S1), 65–70. [[CrossRef](#)]

